



A waterborne polyurethane–based leather finishing agent with excellent room temperature self-healing properties and wear-resistance

Chao Liu¹ · Qing Yin² · Xi Li² · Lifen Hao² · Wenbo Zhang^{1,3} · Yan Bao⁴ · Jianzhong Ma⁴

Received: 21 November 2020 / Revised: 23 December 2020 / Accepted: 4 January 2021 / Published online: 21 January 2021
© The Author(s), under exclusive licence to Springer Nature Switzerland AG part of Springer Nature 2021

Abstract

Water-based polymers have been widely used in coating materials, but their durability and service life are often greatly reduced due to macroscopic damage or cracking caused by external forces. In this paper, poly(propylene glycol) terminated with ortho-amiomethylphenyl diboronic acid (AMPBA-PPG) and cross-linked polymer containing boroxine (CLP-boroxine) were synthesized by nucleophilic substitution. Then the CLP-boroxine was introduced into waterborne polyurethane (WPU) to prepare AMPBA-PPG/WPU composite emulsion for leather finishing and CLP-boroxine/WPU composite film. The self-healing characterization results showed that the self-healing efficiency of the 15 wt% CLP-boroxine/WPU film was as high as 93.6% after only 4 h of water stimulation at room temperature. Compared with neat WPU finished leather, the leather samples finished with AMPBA-PPG/WPU exhibited more excellent wear-resistance. More importantly, the leather coating finished with AMPBA-PPG/WPU still showed nice wear-resistance even after wear and self-healing treatment. These results are attributed to that the hydrogen bonds between AMPBA-PPG and WPU, WPU, and WPU, and the dynamic reversible covalent bonds in AMPBA-PPG can improve/increase the self-healing efficiency of the composite coating. In addition, the boron hydroxyl groups in AMPBA-PPG could also react with the hydroxyl groups on the leather surface, thereby further improving the wear-resistance of the leather coating.

Keywords Waterborne polyurethane · Leather finishing · Self-healing · Wear-resistance

1 Introduction

Waterborne polyurethane (WPU) is a new type of polyurethane system emerging to meet the increasing demand for environment friendly materials all over the world [1]. WPU is widely used as the finishing materials for leather, fabric, wood, rubber, and plastic engineering due to its environmental protection, strong adhesion, and film

forming properties [2–4]. However, due to its poor wear-resistance, the durability and service life of WPU coating are dramatically reduced [5–7]. Therefore, it is an urgent requirement to develop a WPU coating with improved wear-resistance not only to enhance its function as a protective material but also renders its finishing products a higher application value.

Introducing materials with self-healing function into WPU system can endow WPU with self-healing property [8–10]. So, its service life can be effectively improved and its coated products can be endowed with higher application value [11–16]. Reversible covalent bond self-healing system is a healing process using reversible chemical reactions of polymer materials [17], including disulfide bond reaction [18], Diels-Alder reaction [19], imine bond reaction [20], and acylhydrazone bond reaction [21]. The bond energy of reversible covalent bonds is second only to that of covalent bonds, so materials based on reversible covalent bond not only have excellent self-healing properties, but also have superior mechanical

Highlights

- A cross-linked polymer containing boroxine were synthesized.
- The coating finished with AMPBA-PPG/WPU shows nice wear-resistance.
- The CLP-boroxine/WPU films can effectively self-healing at room temperature.

✉ Chao Liu
lc1010158@163.com

✉ Jianzhong Ma
majz@sust.edu.cn

Extended author information available on the last page of the article

properties and wear-resistance [22–25]. Deng et al. [26] prepared a self-healing hydrogel with acylhydrazone bond. The fracture of this hydrogel can be self-healing after 48 h under acidic conditions, and its self-healing efficiency is 90%. Bergman et al. [27] used heat to make the imine group react with furan group on maleamide for DA reaction. Then, the material underwent reversed DA reaction by cooling down to repair the damage. These results indicate that most self-healing materials based on reversible covalent bonds usually require external stimuli such as pH, heat, and light.

The unique molecular structure of boron-oxygen compounds makes polymer materials have higher cross-linking density, which is very suitable for manufacturing polymer materials with high mechanical strength [28–30]. Boric acid/boronate ester balance is easily changed by temperature or the addition/removal of Lewis base or water, thus providing a self-healing mechanism [31, 32]. Lai et al. [33] use dynamic boronate ester bonds to crosslink polydimethylsiloxane chain into the 3D network. The prepared samples could achieve most of the mechanical strength after being heated at 70 °C after wetting and healing for 12 h. Boronate ester is formed by boric acid and diol under alkaline conditions. They are extremely unstable under acidic conditions [34, 35]. Compared with the boric acid center, the presence of an amino group in the ortho position can achieve B–N interactions, thereby reducing the alkalinity of amine and the acidity of boric acid, thus contributing to form boronate ester in a neutral pH value [28, 36, 37]. In addition, boronate ester is a thermally stable dynamic covalent bond. Compared with boronate ester, B–N bonds can reduce the acidity of boric acid; consequently, nitrogen coordinate boronate ester can be broken and re-built reversibly at a relatively low temperature [38, 39]. Therefore, the nitrogen-coordinate boronate ester can make up for the shortage of boronate ester. It can achieve positive self-healing ability of material under the stimulation of water at room temperature.

In this paper, poly(propylene glycol) terminated with ortho-amiomethylphenyl diboronic acid and cross-linked polymer containing boroxine (denoted as AMPBA-PPG and CLP-boroxine) were synthesized by nucleophilic substitution. And then, the CLP-boroxine was introduced into waterborne polyurethane (WPU) and used for the constructing of self-healing and wear-resistant leather coating by utilizing the high reversibility, the cross-linking of boroxines, and rich hydrogen bonding networks. Upon the water stimulation, the CLP-boroxine/WPU composite films could achieve rapid self-healing at room temperature. Meanwhile, the wear-resistance of the CLP-boroxine/WPU composite leather coating had been significantly improved due to the chemical interaction

between boron hydroxyl of CLP-boroxine and hydroxyl groups on the surface of the collagen fiber. What is more worthy of attention was that the composite coating still showed well wear-resistance after the treatment of first wear and then self-healing. These results indicate that the introduction of borate-based dynamic covalent bonds in the coating system can provide a new strategy for constructing self-healing and durable wear-resistant coating on the surface of polyhydroxy-containing substrates.

2 Experimental

2.1 Materials

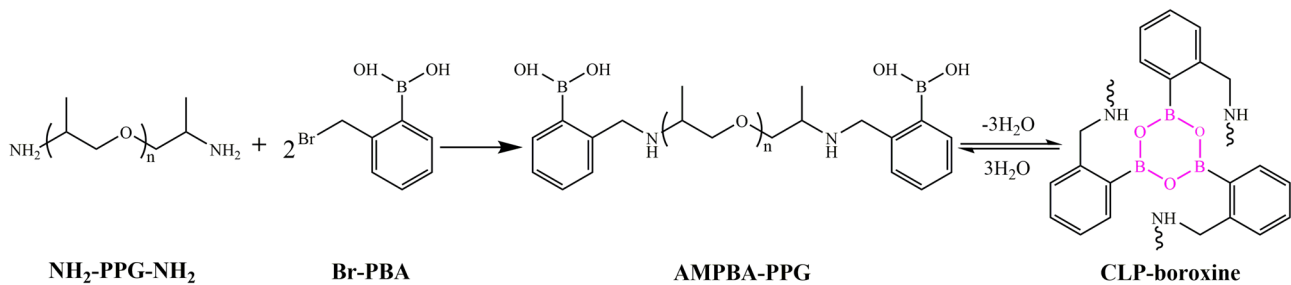
Poly(propylene glycol) bis(2-aminopropyl ether) ($\text{NH}_2\text{-PPG-NH}_2$, $M_n \approx 2000$) and 2-(bromomethyl) phenylboronic acid (Br-PBA) were purchased from Aladdin Industrial Corporation. Isophorone diisocyanate (IPDI), dibutyltin dilaurate (DBTDL), and 2, 2-dihydroxybutyric acid (DMBA) were provided by Shanghai Maclin Biochemical Co., Ltd. and Guangdong Guanghua Sci-Tech Co., Ltd., respectively. Polytetramethylene glycol (PTMG1000) and dichloromethane (CH_2Cl_2 , $\geq 99.5\%$) were procured from Jining Huakai Resin Co., Ltd. Ethanol and triethylamine (TEA, $\geq 99.5\%$) were obtained from Tianjin Fuyu Fine Chemical Co., Ltd. All chemicals were analytical grades and used directly without further processing.

2.2 Preparation of WPU

Firstly, PTMG1000 and IPDI were mixed in a three-neck round-bottom flask (500 mL) and stirred using a mechanical agitator for 30 min. Then, three drops of DBTDL were added to the mixture and continued to stir for 30 min. Afterwards, the water bath was heated to 75 °C for 3 h. Subsequently, DMBA was slowly added to reaction solution as chain extender. The reaction continued for 2 h before being cooled to 50 °C. Finally, TEA (4 mL) was added by pipette and reacted for 20 min, and then deionized water was added and emulsified for 1 h.

2.3 Synthesis of AMPBA-PPG and CLP-boroxine

Br-PBA (1.29 g) and $\text{NH}_2\text{-PPG-NH}_2$ (6 g) were first successively added to a three-necked flask containing 60 mL of ethanol and reacted at 60 °C for 6 h under stirring conditions. Next, the above mixture was placed in an ice water bath, and NaBH_4 (0.37 g) and a drop of acetic acid glacial were slowly added, and the reaction was continued for 2 h. After the reaction was completed,



Scheme 1 Synthesis route of AMPBA-PPG and CLP-boroxine

ethanol was removed by distillation to obtain AMPBA-PPG. Finally, the AMPBA-PPG gradually dehydrated and cross-linked into CLP-boroxine after the drying process was carried out. The synthetic route of AMPBA-PPG and CLP-boroxine is showed in Scheme 1.

2.4 Preparation of CLP-boroxine/WPU composite films

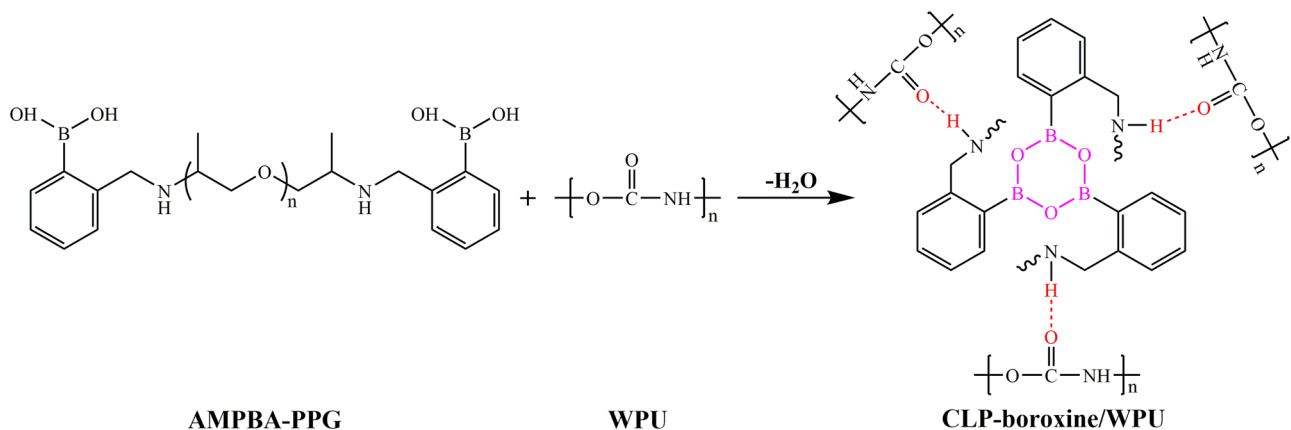
Under magnetic stirring, ethanol solution of CLP-boroxine was added to WPU drop by drop (about a drop in 10 s), and the AMPBA-PPG/WPU composite emulsion was formed by the hydrolysis of CLP-boroxine. CLP-boroxine/WPU composite film was obtained by transferring AMPBA-PPG/WPU composite emulsion into a polytetrafluoroethylene film-forming plate to evaporate the solvent at room temperature for 12 h. During the film formation process, as the solvent evaporates, the hydrogen bond interactions between the secondary amine groups of AMPBA-PPG and the carbonyl groups of the WPU, and the transition from AMPBA-PPG to CLP-boroxine structure promote the formation of multiple network structures inside the composite film (As shown in Scheme 2).

2.5 Application in leather finishing

The WPU and AMPBA-PPG/WPU composite emulsion were employed for leather finishing. Before finishing the leather, the amount of spray required for the leather samples area were calculated according to QB/T 2002.2–2018. Then the specified amount of composite emulsion was mixed with water at a mass ratio of 1:1. After mixing uniformly, the air pressure and the discharge amount of the spray gun were adjusted to be sprayed, and each leather sample was sprayed back and forth repeatedly.

2.6 Characterization

The chemical structure of samples was analyzed by Fourier transform infrared spectroscopy (FT-IR) using a Bruker VERTEX-80 spectrometer in the range of 400–4000 cm^{-1} . Nuclear magnetic resonance spectrometer (^1H NMR) of AMPBA-PPG was measured on a 400-MHz NMR spectrometer at room temperature. In order to analyze the thermal stability of CLP-boroxine, the thermal properties of CLP-boroxine were tested by differential scanning calorimetry (DSC) using



Scheme 2 Preparation route of CLP-boroxine/WPU composite films

a NETZSCH DSC200F3 system. In details, the samples were heated from -80 to 50 °C at a rate of 10 °C/min under a nitrogen flow rate of 50 mL/min. The fracture morphologies of the samples were tested by Hitachi S-4800 field emission scanning electron microscope (SEM). Briefly, the film cross-section was sprayed with gold by JEOL JFC-1600, and the SEM test conditions were an acceleration voltage of 3.0 kV and a current of 10 μ A.

The mechanical properties of the CLP-boroxine/WPU composite films and leather samples were determined using an AI-3000 tensile tester with a stretching rate of 100 mm/min. The CLP-boroxine/WPU composite films were cut into dumbbell shapes with 80 mm in full length, 30 mm in effective length, and 5 mm in intermediate width. Each sample was tested three times.

All the wear experiments in this article were carried out on the MMUD-1B friction and wear testing machine. In the experiment of wear, the end friction pair was carried out by dry friction at room temperature without lubricating oil, and the standard wool felt was fixed on the friction head. The parameters of friction and wear test are as follows: test force is 120 N, rotation speed is 50 r/min, and the test time is 60 min. The detailed information of wear index calculation is available in supplementary information file.

The self-healing ability of CLP-boroxine/WPU composite film was tested at room temperature. The CLP-boroxine/WPU composite film was first cut into two separate films with a bistoury, and the ends of the damaged two sections were immersed in water for 2 min. Then the two sections were butted together at room temperature for 4 h for self-healing. The self-healing efficiency of the

CLP-boroxine/WPU composite film was evaluated by its tensile strength before and after self-healing.

3 Results and discussion

3.1 Characterization of CLP-boroxine

Figure 1 showed the FT-IR results of Br-PBA, CLP-boroxine, and NH_2 -PPG- NH_2 . For Br-PBA, the characteristic peak at 3387 cm^{-1} belongs to the stretching vibrations of B-OH and the peaks at 1596 and 1349 cm^{-1} are attributed to Ar (C=C) and B-O bonds, respectively [40, 41]. With regard to the polymer of NH_2 -PPG- NH_2 , the peak at 1598 cm^{-1} is attributed to the bending vibration of R- NH_2 , while the typical peak at 1105 cm^{-1} is assigned to the formation of C-O-C bonds [42]. In the spectrum of CLP-boroxine, both the peak at 3387 cm^{-1} of B-OH stretching vibration in Br-PBA and the peak at 1598 cm^{-1} of N-H deformation vibration in NH_2 -PPG- NH_2 are disappeared. However, a new peak appears at 750 cm^{-1} , which is attributed to the boroxine [43]. The results confirm that the Br-PBA and NH_2 -PPG- NH_2 have been reacted successfully, and the boroxine structure has formed in CLP-boroxine.

^1H NMR was used to further investigate the chemical structure of AMPBA-PPG. As presented in Fig. 2, the chemical shifts of hydrogen atoms in AMPBA-PPG molecule are in the range of 7.51 – 1.18 ppm, including the following: δ 7.51 ppm (Ha, 2H, Ar-H), δ 7.22 – 7.15 ppm (Hb, 6H, Ar-H), δ 4.89 ppm (Hc, 4H, B-OH), δ 4.07 ppm (Hd, 4H, Ar- CH_2 -), δ 3.88 – 3.84 ppm (He, 2H, -NH-), δ 3.75 – 3.15 ppm (Hf, Hg, 106H, -CH-, - CH_2 -), and δ 1.15 ppm (Hh, 106H, - CH_3). ^1H NMR spectrum further

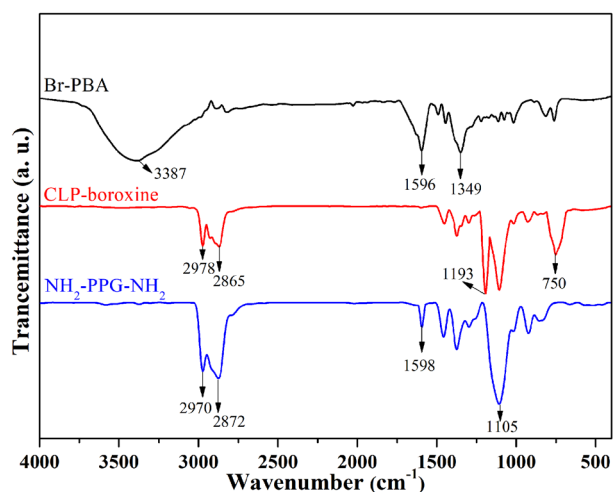


Fig. 1 FT-IR spectra of Br-PBA, NH_2 -PPG- NH_2 , and CLP-boroxine, respectively

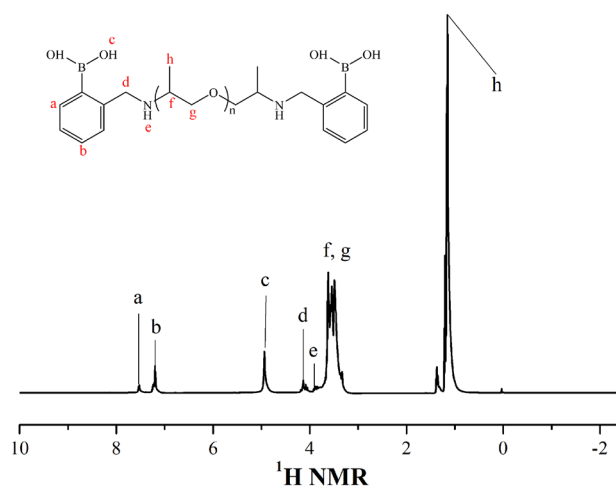


Fig. 2 ^1H NMR spectrum of AMPBA-PPG in CD_3OD



Fig. 3 Inclined **a** and inverted **b** views of the CLP-boroxine in vial, and DSC curves **c** of CLP-boroxine at $-80\text{ }^{\circ}\text{C}$ – $50\text{ }^{\circ}\text{C}$

demonstrates that the AMPBA-PPG has been synthesized successfully.

CLP-boroxine was put into a small vial, and its appearance was shown in Fig. 3. As can be seen in Fig. 3, the CLP-boroxine is a transparent yellowish color and shows good fluidity at room temperature. Figure 3c is the DSC curve of the CLP-boroxine. The DSC curve shows the glass transition temperature (T_g) of CLP-boroxine is $-70\text{ }^{\circ}\text{C}$. Moreover, the two critical points indicate that it is in glassy state before $-75\text{ }^{\circ}\text{C}$, in viscous flow state after $-53\text{ }^{\circ}\text{C}$ [44, 45]. Therefore, CLP-boroxine exhibits a viscous flow state at room temperature. This result has an agreement with the observation as shown in Fig. 3b. All these results indicate that CLP-boroxine is more easily incorporated into emulsion systems.

3.2 Properties of AMPBA-PPG/WPU composite emulsion and CLP-boroxine/WPU composite films

The Zeta potential of AMPBA-PPG and WPU emulsion is characterized by nano particle surface potential analyzer for studying the stability of AMPBA-PPG/WPU composite emulsion. Table 1 showed that the Zeta potentials of AMPBA-PPG and WPU emulsion are -11.3 mV and -34.9 mV at $\text{pH}=7$, respectively. This result indicates that there is a repulsive effect between them. This repulsion separates AMPBA-PPG from WPU, which is conducive to the stability of the emulsion [46]. Therefore, the addition of AMPBA-PPG to WPU emulsion can maintain the stability of its composite emulsion.

Table 1 Zeta potential of AMPBA-PPG and WPU

Samples	Zeta potential (mV)
AMPBA-PPG	-11.3
WPU	-34.9

To further illustrate its storage stability, AMPBA-PPG is added into WPU emulsion and the resulted mixture is kept still at room temperature for 20 days to observe the status of the composite emulsion. The results show that the composite emulsion remains stable and shows even dispersion after 20 days at room temperature. Moreover, AMPBA-PPG/WPU composite emulsion (10 g) has been centrifuged at 3000 r/min for 30 min for the purpose of testing its centrifugal stability. The results show that the AMPBA-PPG/WPU composite emulsion has no obvious precipitation, gelation or stratification, etc. (As shown in Fig. 4). This phenomenon indicates that the centrifugal stability of AMPBA-PPG/WPU composite emulsion is splendid [47, 48]. In summary, the AMPBA-PPG/WPU composite emulsion has excellent stability.

The FT-IR spectra were used to characterize the chemical structure of CLP-boroxine/WPU composite film (Fig. 5). The FT-IR spectrum of CLP-boroxine/WPU composite film shows that the C=O stretching vibration peak in WPU changes from 1706 cm^{-1} to 1745 cm^{-1} , and the peak at 1589 cm^{-1} corresponding to the -NH group shifts to 1542 cm^{-1} in the CLP-boroxine. These are attributed to the formation of hydrogen bonds between the carbonyl groups of WPU and the secondary amine groups of CLP-boroxine in CLP-boroxine/WPU composite films [49, 50]. At the same time, the absorption peak of boroxine

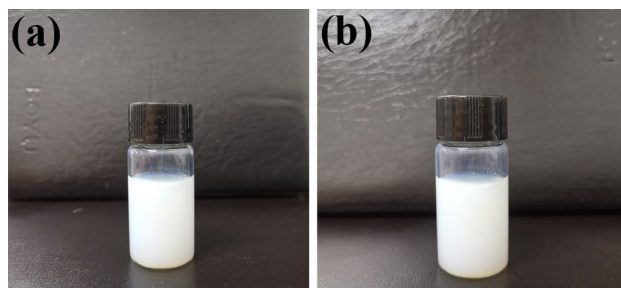


Fig. 4 Visual appearance of AMPBA-PPG/WPU composite emulsion **a** without and **b** after centrifugation at 3000 r/min for 30 min

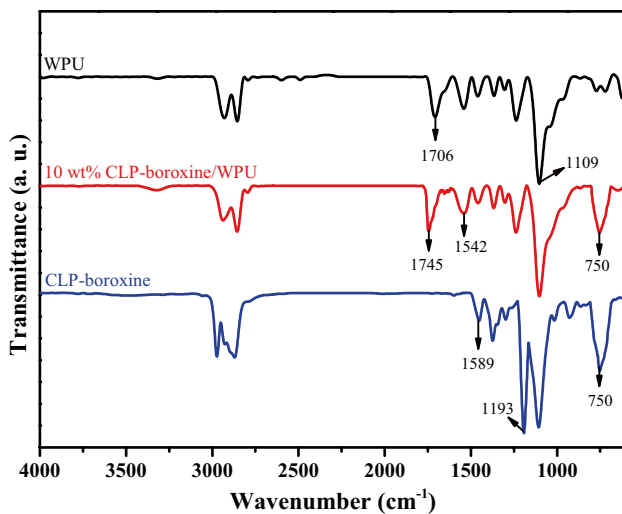


Fig. 5 FT-IR spectra of WPU, CLP-boroxine, and 10 wt% CLP-boroxine/WPU, respectively

appears at 750 cm^{-1} , which indicates that CLP-boroxine/WPU composite films are formed.

3.3 Mechanical properties of CLP-boroxine/WPU composite films

The tensile strength and elongation at break of CLP-boroxine/WPU composite films with different CLP-boroxine contents as can be seen in Fig. 6. It can be clearly seen in Fig. 6a that the tensile strength of CLP-boroxine/WPU composite films decreases continuously with the addition of CLP-boroxine. This phenomenon that may be attributed to the CLP-boroxine is a flexible

material. The CLP-boroxine may reduce the strength of the films when added to WPU.

As for the elongation at break, Fig. 6b shows different tendency compared with tensile strength of CLP-boroxine/WPU composite films. It can be seen that a suitable amount of CLP-boroxine can greatly increase the elongation at break of WPU film. Its elongation at break reaches the maximum value of 731.2% with 10 wt% CLP-boroxine, an increase of as much as 23.8% in comparison with that of the neat WPU film (590.5%). This may be attributed to two reasons. On the one hand, rich hydrogen bonds have been formed between the secondary amine groups of CLP-boroxine and the carbonyl groups of WPU, thus effectively enhancing the interaction between molecular chains. On the other hand, multiple network structures can be formed in the composite system through the production of boronate ester bonds between CLP-boroxine, thereby enhancing the strength of the molecular chains of the CLP-boroxine/WPU composite system.

In order to explain this phenomenon, the fracture surface morphologies of neat WPU and CLP-boroxine/WPU composite films after tensile tests were studied by SEM, which provided immediate proof for the interfacial interactions between CLP-boroxine and WPU (Fig. S1). While with the further increase of the CLP-boroxine addition, the elongation at break of CLP-boroxine/WPU composite film decreases. This may be due to the fact that CLP-boroxine itself is an ultra-low strength material. Too much addition will not only reduce the strength of the CLP-boroxine/WPU composite film but also reduce the interaction between molecules [30].

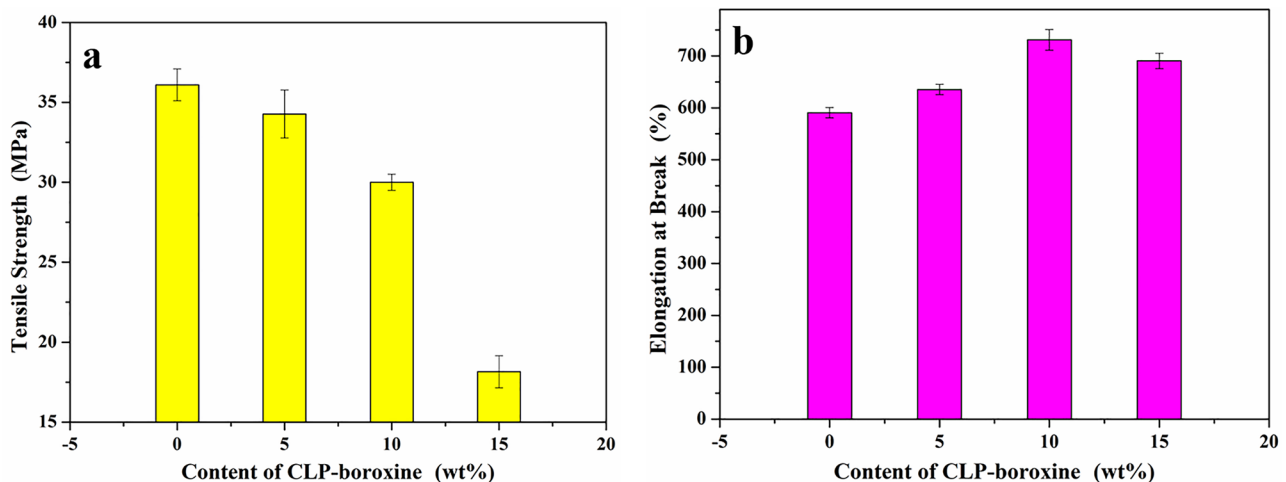
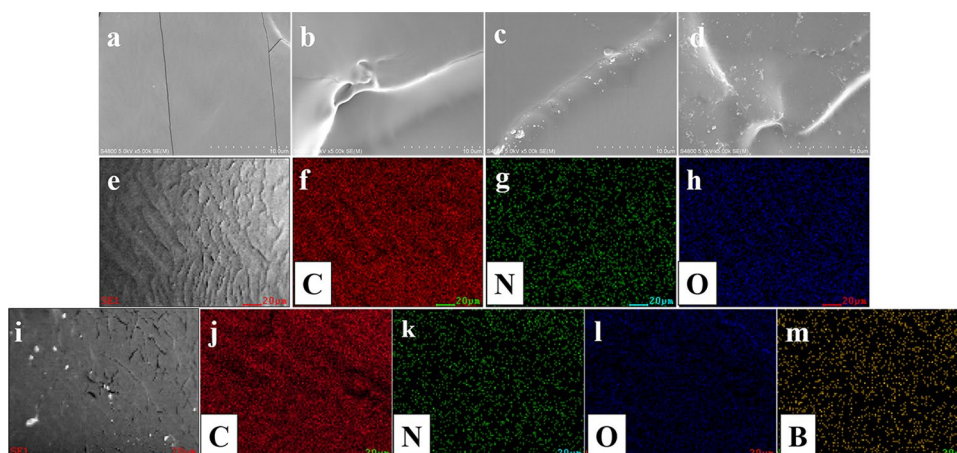


Fig. 6 **a** Tensile strength and **b** elongation at break of CLP-boroxine/WPU composite films with different CLP-boroxine contents

Fig. 7 SEM micrograph of fractured surface of CLP-boroxine/WPU composite films obtained with the different content of CLP-boroxine. **a** 0 wt%, **b** 5 wt%, **c** 10 wt%, **d** 15 wt%, and EDX mapping of **e–h** neat WPU and **i–m** 10 wt% CLP-boroxine/WPU. Red, green blue, and yellow dots indicate signals of C, N, O, and B, respectively



3.4 Analysis of section morphology of CLP-boroxine/WPU composite films

In order to observe the internal structure of CLP-boroxine/WPU composite films, the films with different CLP-boroxine contents were brittle fractured with liquid nitrogen (as shown in Fig. 7). It can be seen that the morphology fractured surface of the neat WPU film is relatively smooth. Cracks appear on the fractured surface of neat WPU, which is the result of liquid nitrogen freezing. As the amount of CLP-boroxine increases, there is no crack on the fractured surface of CLP-boroxine/WPU composite film, which indicates that CLP-boroxine has better low temperature resistance. Meanwhile, a large number of white substances appear on the fractured surface of CLP-boroxine/WPU composite film. These white substances may be the aggregates of precipitated CLP-boroxine. This may be due to the fact that the condensation of water vapor on the fractured surface of composite film leading to the transformation from CLP-boroxine to AMPBA-PPG and then precipitate from the matrix. As water vapor evaporates, the AMPBA-PPG accumulates and transforms CLP-boroxine compound gel on the fractured surface of composite film [51]. The EXD mapping of 10 wt% CLP-boroxine/WPU (Fig. 7e–m) is further confirmed that CLP-boroxine is uniformly distributed in the CLP-boroxine/WPU composite film.

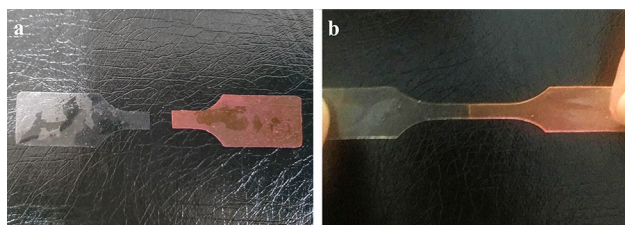


Fig. 8 Comparison of 15 wt% CLP-boroxine/WPU composite film before **a** and after **b** healing

3.5 Self-healing ability of CLP-boroxine/WPU composite films

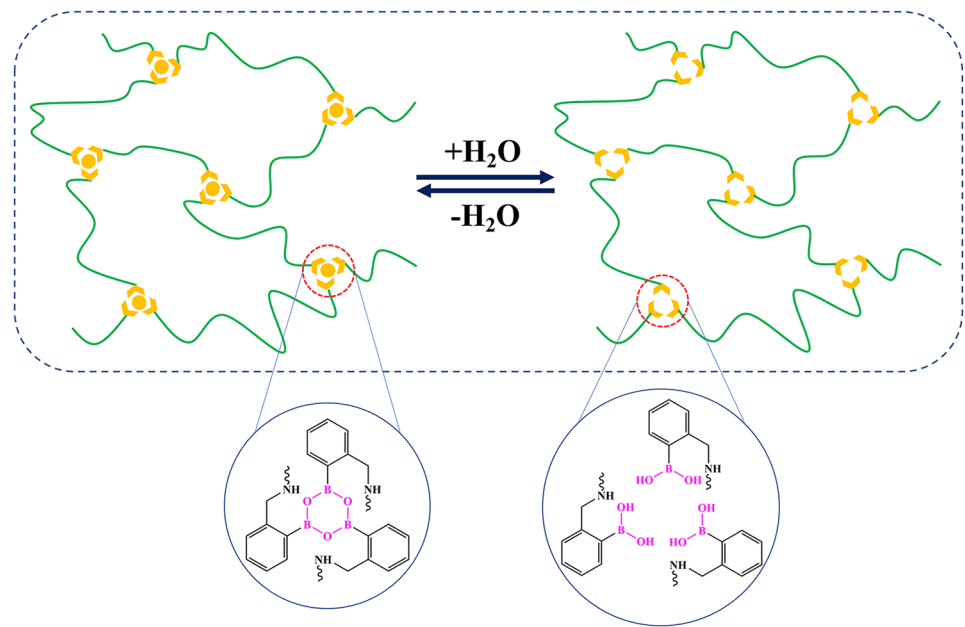
The CLP-boroxine/WPU composite films possess good self-healing property by virtue of the dynamic reversibility of boronate ester bond in the presence of water at room temperature. As can be seen in Fig. 8, the incision in the 15 wt% CLP-boroxine/WPU composite film has been completely healed under water stimulation at room temperature for 4 h. This primary proves that the CLP-boroxine/WPU composite film has self-healing property by direct visual method. Boronate ester group is responsive to water stimulation. So, the water resistance of CLP-boroxine/WPU composite films is discussed (see Fig. S2). Compared with the neat WPU film, the water resistance of the 5 wt% CLP-boroxine/WPU composite film is significantly improved. However, when the amount of CLP-boroxine added exceeds 5 wt%, the water absorption of CLP-boroxine/WPU composite films is increased. This phenomenon that may be attributed to the presence of excessive CLP-boroxine in the system will hinder the interaction between WPU molecules, resulting in changes in the densification of CLP-boroxine/WPU composite films.

In order to further evaluate the self-healing performance of the CLP-boroxine/WPU composite films, tensile testing

Table 2 The self-healing efficiency of different content of CLP-boroxine/WPU composite films

Content of CLP-boroxine (wt%)	Tensile strength (MPa)	Tensile strength after self-healing (MPa)	Self-healing efficiency (%)
0	36.10	6.33	17.52
5	34.27	23.18	67.63
10	30.00	24.68	82.27
15	18.15	16.99	93.59

Fig. 9 The healing mechanism of CLP-boroxine/WPU composite films



is carried out on the self-healed samples with different CLP-boroxine content. Table 2 indicates that neat WPU film also has self-healing ability, which is mainly due to the large amount of intermolecular hydrogen bonding in WPU. But the healing efficiency of it is only 17.52%. Compared with neat WPU, the self-healing efficiency of CLP-boroxine/WPU increases with the introduction CLP-boroxine. When the CLP-boroxine amount is 15%, the self-healing efficiency of CLP-boroxine/WPU composite film is as high as 93.59%.

The excellent self-healing performance of CLP-boroxine/WPU composite film is mainly attributed to three aspects.

On the one hand, CLP-boroxine itself has better molecular chain flexibility. The introduction of CLP-boroxine into WPU can improve the molecular motion ability. On the other hand, the hydrogen bond between WPU and CLP-boroxine and the dispersion of WPU itself can promote the rapid aggregation of molecular chains [52]. Therefore, the speed of self-healing is accelerated. On the last aspect, multiple network structure of boronate ester bond is formed with the evaporation of water, thereby realizing self-healing function of CLP-boroxine/WPU. The healing mechanism of it is shown in Fig. 9.

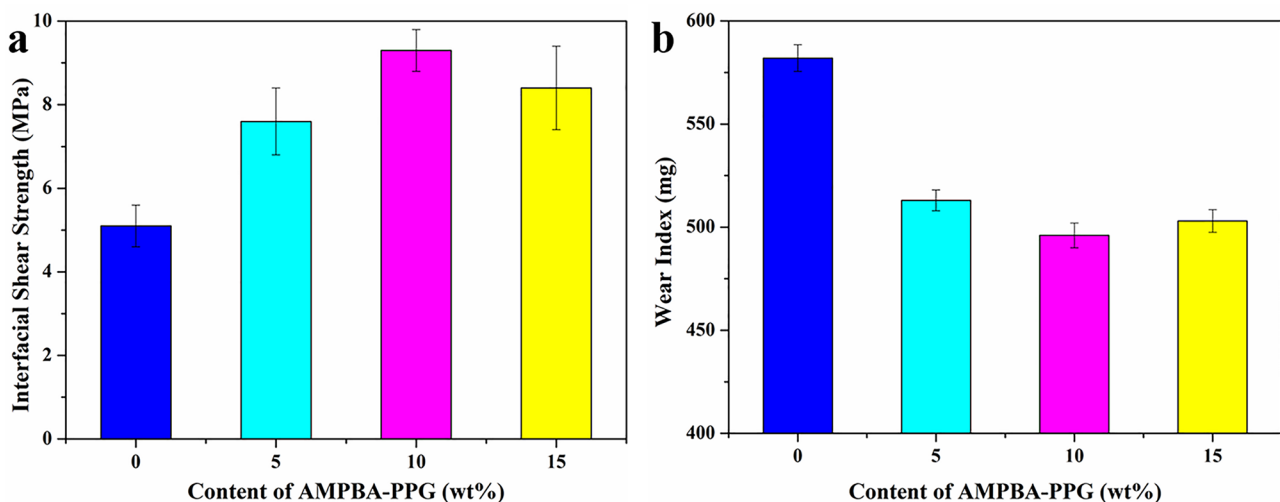


Fig. 10 **a** Interfacial shear strength and **b** wear index of AMPBA-PPG/WPU composite emulsion coated leather samples with different AMPBA-PPG content

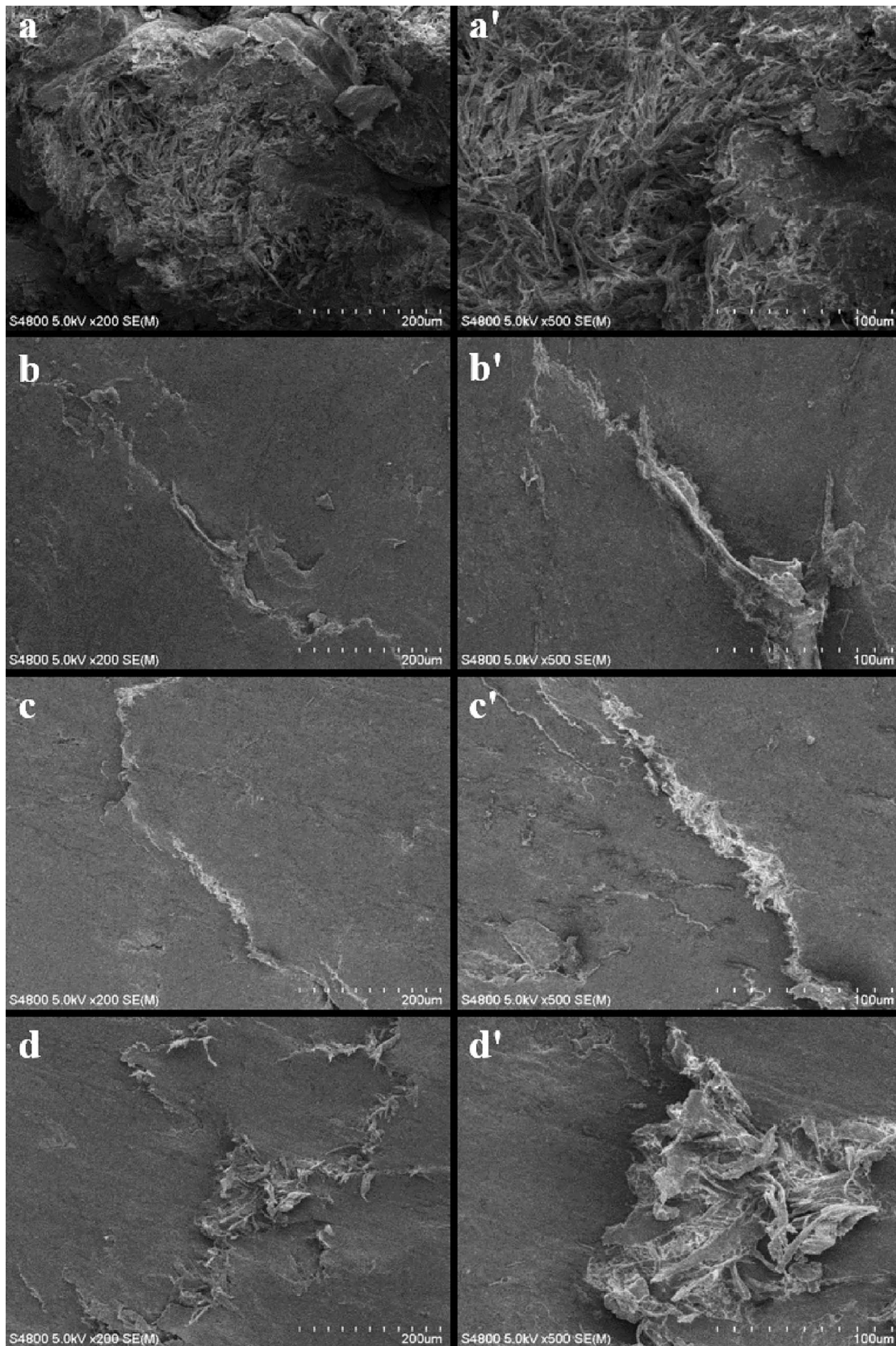


Fig. 11 SEM images of worn surface of unfinished leather **a–a'**, the leather samples coated by WPU **b–b'**, 15 wt% AMPBA-PPG/WPU (**c–c'**), and the leather sample coated by 15 wt% AMPBA-PPG/WPU after wear and healing treatment **d–d'**, respectively

In addition, in order to further study the healing properties of the composite films, the healing efficiency of 15 wt% CLP-boroxine/WPU composite film with different healing times was also analyzed. As shown in Fig. S3, the healing efficiency of 15 wt% CLP-boroxine/WPU composite film gradually increases with the extension of healing time. However, when the self-healing time exceeded 4 h, there is no significant change in the self-healing efficiency. This phenomenon that may due to the system has reached a relative balance after 4 h of self-healing treatment.

3.6 Applied properties of AMPBA-PPG/WPU composite emulsion for leather finishing

In order to further study the application performance of AMPBA-PPG/WPU composite emulsion, the as-prepared composite emulsion has been applied to leather finishing. The AMPBA-PPG/WPU composite emulsion would form a coating film on the surface of leather after drying, which plays a variety of applications such as beautify leather surface, hide leather surface defects, and improve the performance of leather [53]. The tribological properties of AMPBA-PPG/WPU composite coating were studied by wear-resistance test. Compared with neat WPU (582 mg), the wear index of AMPBA-PPG/WPU finished leather samples reduced by 11.8~15.9% (69~93 mg) with different contents of AMPBA-PPG (As shown in Fig. 10b). This result indicates that AMPBA-PPG/WPU coating can effectively improve the wear-resistance of leather.

In order to further evaluate the protection of the AMPBA-PPG/WPU coating, SEM was used to observe the surface of the coated leather after abrasion. As revealed in Fig. 11, the leather samples coated with WPU and AMPBA-PPG/WPU composite coating agent have a relatively good protection function. The uncoated leather sample is severely worn and exposed to a large amount of collagen fibers, as shown in Fig. 11a–a'. However, WPU and 15 wt% AMPBA-PPG/WPU finished leather samples show only slight wear of the coating after friction, and no significant exposure of the collagen fibers are observed (Fig. 11b–c'). It is worth noting that the leather samples finished with 15 wt% AMPBA-PPG/WPU still show excellent wear-resistance after self-healing (Fig. 11d–d'). The unique self-healing function of AMPBA-PPG/WPU coating can effectively extend its wear-resistant life. The excellent wear-resistance of AMPBA-PPG/WPU coating that may be attributed to the boron hydroxyl groups in AMPBA-PPG can react with the hydroxyl groups on the surface of leather collagen fiber, thus effectively improving the adhesive property of AMPBA-PPG/WPU coating (Fig. 10a).

4 Conclusions

In this paper, a novel of AMPBA-PPG/WPU composite coating with water-induced self-healing function was prepared by a blending method. With the increase of CLP-boroxine content, the tensile strength of CLP-boroxine/WPU composite films gradually decreases, while the elongation at break increases first and then decreases. With the increase of CLP-boroxine content, the healing efficiency of the CLP-boroxine/WPU composite films increases gradually and reaches 93.6% after 4 h self-healing at room temperature (15 wt% CLP-boroxine/WPU). Compared with neat WPU finished leather samples, the leather samples finished with AMPBA-PPG/WPU exhibit more excellent wear-resistance. This is mainly due to the fact that AMPBA-PPG can form chemical bond with collagen fibers on the surface of leather, thus effectively improving the wear-resistance and adhesion of the composite coating. And even more remarkable, the leather coating finished with AMPBA-PPG/WPU still show nice wear-resistance even after wear and self-healing treatment. This work provides a new approach to the development of leather coatings with durable wear-resistance.

Supplementary Information The online version contains supplementary material available at <https://doi.org/10.1007/s42114-021-00206-3>.

Funding This work was supported by the National Natural Science Foundation of China (Grant Numbers 22008145, 22078188), the Natural Science Basic Research Plan in Shaanxi Province of China (Grant Number 2018JQ5211), and the Basic Industrial Science and Technology Projects of Wenzhou (Grant Number G20190008).

Compliance with ethical standards

Conflict of interest The authors declare that they have no conflict of interest.

References


1. Ren W, Zhu HX, Yang YQ, Chen YH, Duan HJ, Zhao GZ, Liu YQ (2020) Flexible and robust silver coated non-woven fabric reinforced waterborne polyurethane films for ultra-efficient electromagnetic shielding. *Compos Part B* 184:107745
2. Wang J, Ye L (2015) Structure and properties of polyvinyl alcohol/polyurethane blends. *Compos Part B* 69:389–396
3. Kang SY, Ji ZX, Tseng LF, Turner SA, Villanueva DA, Johnson R, Albano A, Langer R (2018) Design and synthesis of waterborne polyurethanes. *Adv Mater* 30(18):1706237
4. Gu H, Liu C, Zhu J, Gu JW, Guo ZH (2018) Introducing advanced composites and hybrid materials. *Adv Compos Hybrid Mater* 1(1):1–5
5. Wang T, Yu WC, Zhou CG, Sun WJ, Li ZM (2020) Self-healing and flexible carbon nanotube/polyurethane composite for efficient electromagnetic interference shielding. *Compos Part B* 193:108015

6. Chen J, Huang Y, Ma X, Lei Y (2017) Functional self-healing materials and their potential applications in biomedical engineering. *Adv Compos Hybrid Mater* 1(1):94–113
7. Kim SY, Jones AR, Sottos NR, White SR (2017) Manufacturing of unidirectional glass/epoxy prepreg with microencapsulated liquid healing agents. *Compos Sci Technol* 153:190–197
8. Wan T, Chen DJ (2018) Preparation of β -cyclodextrin reinforced waterborne polyurethane nanocomposites with excellent mechanical and self-healing property. *Compos Sci Technol* 168:55–62
9. Huynh TP, Sonar P, Haick H (2017) Advanced materials for use in soft self-healing devices. *Adv Mater* 29(19):1604973
10. Li CH, Wang C, Keplinger C, Zuo JL, Jin LH, Sun Y, Zheng P, Cao Y, Lissel F, Linder C, You XZ, Bao ZN (2016) A highly stretchable autonomous self-healing elastomer. *Nat Chem* 8(6):618
11. Fang YL, Du XS, Jiang YX, Du ZL, Pan PT, Cheng X, Wang HB (2018) Thermal-driven self-healing and recyclable waterborne polyurethane films based on reversible covalent interaction. *ACS Sustainable Chem Eng* 6(11):14490–14500
12. Yang XT, Guo YQ, Luo X, Zheng N, Ma TB, Tan JJ, Li CM, Zhang QY, Gu JW (2018) Self-healing, recoverable epoxy elastomers and their composites with desirable thermal conductivities by incorporating BN fillers via in-situ polymerization. *Compos Sci Technol* 164:59–64
13. Li CM, Tan JJ, Gu JW, Qiao L, Zhang BL, Zhang QY (2016) Rapid and efficient synthesis of isocyanate microcapsules via thiol-ene photopolymerization in pickering emulsion and its application in self-healing coating. *Compos Sci Technol* 123:250–258
14. Baltzis D, Paipetis AS, Bekas DG, Tsirka K (2016) Self-healing materials: a review of advances in materials, evaluation, characterization and monitoring techniques. *Compos Part B* 87:92–119
15. Yang XT, Zhong X, Zhang JL, Gu JW (2021) Intrinsic high thermal conductive liquid crystal epoxy film simultaneously combining with excellent intrinsic self-healing performance. *J Mater Sci Technol* 68(30):209–215
16. Gu JW, Yang XT, Li CM, Kou KC (2016) Synthesis of cyanate ester microcapsules via solvent evaporation technique and its application in epoxy resins as a healing agent. *Ind Eng Chem Res* 55(41):10941–10946
17. Fan LF, Rong MZ, Zhang MQ, Chen XD (2018) Repeated intrinsic self-healing of wider cracks in polymer via dynamic reversible covalent bonding molecularly combined with a two-way shape memory effect. *ACS Appl Mater Inter* 10(44):38538–38546
18. Xu YR, Chen DJ (2016) A novel self-healing polyurethane based on disulfide bonds. *Macromol Chem Phys* 217(10):1191–1196
19. Turkenburg DH, Durant Y, Fischer H (2017) Bio-based self-healing coatings based on thermo-reversible Diels-Alder reaction. *Prog Org Coat* 111:38–46
20. Xu CH, Cao LM, Lin BF, Liang XQ, Chen YK (2016) Design of self-healing supramolecular rubbers by introducing ionic cross-links into natural rubber via a controlled vulcanization. *ACS Appl Mater Inter* 8(27):17728–17737
21. Deng RH, Derry MJ, Mable CJ, Ning Y, Armes SP (2017) Using dynamic covalent chemistry to drive morphological transitions: controlled release of encapsulated nanoparticles from block copolymer vesicles. *J AM Chem Soc* 139(22):7616–7623
22. Kang JH, Tok JBH, Bao ZN (2019) Self-healing soft electronics. *Nat Electron* 2(4):144–150
23. Liu J, Ma XN, Tong YP, Lang MD (2018) Self-healing polyurethane based on ditelluride bonds. *Appl Surf Sci* 455:318–325
24. Du WN, Jin Y, Shi LJ, Shen YC, Lai SQ, Zhou YT (2020) NIR-light-induced thermoset shape memory polyurethane composites with self-healing and recyclable functionalities. *Compos Part B* 195:108092
25. Pettignano A, Häring M, Bernardi L, Tanchoux N, Quignard F, Díaz DD (2017) Self-healing alginate-gelatin biohydrogels based on dynamic covalent chemistry: elucidation of key parameters. *Mater Chem Front* 1(1):73–79
26. Deng GH, Li FY, Yu HX, Liu FY, Liu CY, Sun WX, Jiang HF, Chen YM (2012) Dynamic hydrogels with an environmental adaptive self-healing ability and dual responsive sol-gel transitions. *ACS Macro Lett* 1(2):275–279
27. Bergman SD, Wudl F (2008) Mendable polymers. *J Mater Chem* 18(1):41–62
28. Guo RW, Su Q, Zhang JW, Dong AJ, Lin CG, Zhang JH (2017) Facile access to multisensitive and self-healing hydrogels with reversible and dynamic boronic ester and disulfide linkages. *Biomacromol* 18(4):1356–1364
29. Cash JJ, Kubo T, Dobbins DJ, Sumerlin BS (2018) Maximizing the symbiosis of static and dynamic bonds in self-healing boronic ester networks. *Polym Chem* 9(15):2011–2020
30. Bao CY, Jiang YJ, Zhang HY, Lu XY, Sun JQ (2018) Room-temperature self-healing and recyclable tough polymer composites using nitrogen-coordinated boroxines. *Adv Funct Mater* 28(23):1800560
31. Li WT, Dong BQ, Yang ZX, Xu J, Chen Q, Li HX, Xing F, Jiang ZW (2018) Recent advances in intrinsic self-healing cementitious materials. *Adv Mater* 30(17):1705679
32. Hu Z, Zhang DY, Lu F, Yuan WH, Xu XR, Zhang Q, Liu H, Shao Q, Guo ZH, Huang YD (2018) Multistimuli-responsive intrinsic self-healing epoxy resin constructed by host-guest interactions. *Macromolecules* 51(14):5294–5303
33. Lai JC, Mei JF, Jia XY, Li CH, You XZ, Bao ZN (2016) A stiff and healable polymer based on dynamic-covalent boroxine bonds. *Adv Mater* 28(37):8277–8282
34. Bao CY, Guo ZW, Sun HX, Sun JQ (2019) Nitrogen-coordinated boroxines enable the fabrication of mechanically robust supramolecular thermosets capable of healing and recycling under mild conditions. *ACS Appl Mater Inter* 11(9):9478–9486
35. Delpierre S, Willocq B, Winter JD, Dubois P, Gerbaux P, Raquez JM (2017) Dynamic iminoboronate-based boroxine chemistry for the design of ambient humidity-sensitive self-healing polymers. *Chemistry* 23(28):6730–6735
36. Li YS, Yang L, Zeng Y, Wu YW, Wei Y, Tao L (2019) Self-healing hydrogel with a double dynamic network comprising imine and borate ester linkages. *Chem Mater* 31(15):5576–5583
37. Pan FP, Xiang XM, Li Y (2018) Nitrogen coordinated single atomic metals supported on nanocarbons: a new frontier in electrocatalytic CO₂ reduction. *Eng Sci* 1:21–32
38. Tarus D, Hachet E, Messenger L, Catargi B, Ravaine V, Auzély-Velty R (2014) Readily prepared dynamic hydrogels by combining phenyl boronic acid- and maltose-modified anionic polysaccharides at neutral pH. *Macromol Rapid Commun* 35(24):2089
39. Guan Y, Zhang YJ (2013) Boronic acid-containing hydrogels: synthesis and their applications. *Chem Soc Rev* 42(20):8106–8121
40. Liu C, Lin Y, Dong YF, Wu YK, Bao Y, Yan HX, Ma JZ (2020) Fabrication and investigation on Ag nanowires/TiO₂ nanosheets/graphene hybrid nanocomposite and its water treatment performance. *Adv Compos Hybrid Mater* 3(3):402–414
41. Elshaarani T, Yu HJ, Wang L, Abdin Z, Ullah RS, Haroon M, Khan RU, Fahad S, Khan A, Nazir A, Usman M, Naveed K (2018) Synthesis of hydrogel-bearing phenylboronic acid moieties and their applications in glucose sensing and insulin delivery. *J Mater Chem B* 6(23):3831–3854
42. Fielden SDP, Leigh DA, McTernan CT, Pérez-Saavedra B, Vitorica-Yrezabal IJ (2018) Spontaneous assembly of rotaxanes from a primary amine, crown ether and electrophile. *J AM Chem Soc* 140(19):6049–6052
43. Yue JY, Mo YP, Li SY, Dong WL, Chen T, Wang D (2017) Simultaneous construction of two linkages for the on-surface synthesis of imine-boroxine hybrid covalent organic frameworks. *Chem Sci* 8(3):2169–2174

44. Wei Y, Liu CQ, Qiu L, Zhang P, Ma WG, Yue YN, Xie HQ, Larkin LS (2018) Advanced thermal interface materials for thermal management. *Eng Sci* 2:1–3
45. Yu B, Li XT, An JL, Jiang ZY, Yang JL (2018) Interfacial and glass transition properties of surface-treated carbon fiber reinforced polymer composites under hygrothermal conditions. *Eng Sci* 2:67–73
46. Dawoud AM, Jan V, Matthew DJ (2017) Zeta potential of artificial and natural calcite in aqueous solution. *Adv Colloid Interface Sci* 240:60–76
47. Liang CB, Ruan KP, Zhang YL, Gu JW (2020) Multifunctional flexible electromagnetic interference shielding AgNWs/cellulose films with excellent thermal management and joule heating performances. *ACS Appl Mater Inter* 12(15):18023–18031
48. Amalraj A, Raj KJ, Haponiuk JT, Thomas S, Gopi S (2020) Preparation, characterization, and antimicrobial activity of chitosan/gum arabic/polyethylene glycol composite films incorporated with black pepper essential oil and ginger essential oil as potential packaging and wound dressing materials. *Adv Compos Hybrid Mater* 3(4):485–497
49. Liang CB, Liu YX, Ruan YF, Qiu H, Song P, Kong J, Zhang HB, Gu JW (2020) Multifunctional sponges with flexible motion sensing and outstanding thermal insulation for superior electromagnetic interference shielding. *Compos Part A-Appl S* 139:106143
50. Wu JR, Chen DJ (2018) Synthesis and characterization of waterborne polyurethane based on aliphatic diamine sulphonate and liquefiable dimethylol propionic acid. *Prog Org Coat* 118:116–121
51. Tang L, Zhang JL, Gu JW (2020) Random copolymer membrane coated PBO fibers with significantly improved interfacial adhesion for PBO fibers/cyanate ester composites. *Chinese J Aeronaut*. <https://doi.org/10.1016/j.cja.2020.03.007>
52. Ashok RB, Srinivasa CV, Basavaraju B (2019) Dynamic mechanical properties of natural fiber composites—a review. *Adv Compos Hybrid Mater* 106:149–159
53. Li Y, Yi X, Yu T, Xian G (2018) An overview of structural-functional-integrated composites based on the hierarchical microstructures of plant fibers. *Adv Compos Hybrid Mater* 1(3):231–246

Publisher's Note Springer Nature remains neutral with regard to jurisdictional claims in published maps and institutional affiliations.

Affiliations

Chao Liu¹  · Qing Yin² · Xi Li² · Lifen Hao² · Wenbo Zhang^{1,3} · Yan Bao⁴ · Jianzhong Ma⁴

¹ Shaanxi Collaborative Innovation Center of Industrial Auxiliary Chemistry and Technology, Shaanxi University of Science & Technology, Xi'an 710021, China

² College of Chemistry and Chemical Engineering, Shaanxi University of Science & Technology, Xi'an 710021, China

³ Shaanxi Research Institute of Agricultural Products Processing Technology, Xi'an 710021, China

⁴ College of Bioresources Chemical and Materials Engineering, Shaanxi University of Science & Technology, Xi'an 710021, China